Loss of the golgin GM130 causes Golgi disruption, Purkinje neuron loss, and ataxia in mice

Chunyi Liu[a,b,1], Mei Mei[a,1], Qiuling Li[a,1], Peristera Roboti[c], Qianqian Pang[a,b], Zhengzhou Ying[a,b], Fei Gao[d], Martin Lowe[c,2], and Shilai Bao[a,b,2]

[a]State Key Laboratory of Molecular Developmental Biology, Institute of Genetics and Developmental Biology, Chinese Academy of Sciences, Beijing 100101, China; [b]School of Life Sciences, University of Chinese Academy of Sciences, Beijing 100049, China; [c]Faculty of Biology, Medicine and Health, University of Manchester, Manchester M13 9PT, United Kingdom; and [d]State Key Laboratory of Stem Cell and Reproductive Biology, Institute of Zoology, Chinese Academy of Sciences, Beijing 100101, China

Edited by Jennifer Lippincott-Schwartz, Howard Hughes Medical Institute, Ashburn, VA, and approved November 28, 2016 (received for review May 27, 2016)

The Golgi apparatus lies at the heart of the secretory pathway where it is required for secretory trafficking and cargo modification. Disruption of Golgi architecture and function has been widely observed in neurodegenerative disease, but whether Golgi dysfunction is causal with regard to the neurodegenerative process, or is simply a manifestation of neuronal death, remains unclear. Here we report that targeted loss of the golgin GM130 leads to a profound neurological phenotype in mice. Global KO of mouse GM130 results in developmental delay, severe ataxia, and postnatal death. We further show that selective deletion of GM130 in neurons causes fragmentation and defective positioning of the Golgi apparatus, impaired secretory trafficking, and dendritic atrophy in Purkinje cells. These cellular defects manifest as reduced cerebellar size and Purkinje cell number, leading to ataxia. Purkinje cell loss and ataxia first appear during postnatal development but progressively worsen with age. Our data therefore indicate that targeted disruption of the mammalian Golgi apparatus and secretory traffic results in neuronal degeneration in vivo, supporting the view that Golgi dysfunction can play a causative role in neurodegeneration.

GM130 | Golgi apparatus | polarized secretion | Purkinje cell | ataxia

As an important compartment of the endomembrane system, the Golgi apparatus is present in all eukaryotic cells. The Golgi apparatus lies at the heart of the secretory pathway and plays a critical role in the posttranslational modification and trafficking of secretory cargo proteins and lipids (1). In addition to these core functions, the Golgi apparatus also contributes to cell cycle regulation and cytoskeletal dynamics (2–4). The Golgi apparatus has a characteristic architecture, comprising one or more stacks of cisternae that in vertebrate cells are laterally connected to form the Golgi ribbon (5, 6). The vertebrate Golgi is typically positioned adjacent to the centrosome, a localization that is dependent upon interactions with microtubules and the microtubule motor protein dynein (7). In migrating cells or in polarized cells such as neurons, the Golgi is positioned toward the leading edge or apical dendrite, respectively, allowing polarized delivery of secretory cargo to these plasma membrane domains (8–10). In developing neurons, the Golgi can also exist as noncentrosomally associated outposts, thought to be important for localized delivery of cargo direct to the newly forming dendritic plasma membrane as well as local microtubule nucleation to support dendrite morphogenesis (11–14).

Although the Golgi apparatus is well characterized at the molecular level, its roles in development and in tissue homeostasis, and how its dysfunction contributes to disease, remain relatively poorly characterized. For example, we know that the Golgi apparatus undergoes fragmentation in many neurodegenerative diseases, including Alzheimer's disease, Parkinson's disease, amyotrophic lateral sclerosis (ALS), and spinocerebellar ataxia type 2 (SCA2) (15–19). However, whether Golgi fragmentation or impairment of secretory traffic in neurons can cause neurodegeneration, or simply reflects a consequence of cell death, remains unclear (20). Several studies have shown that polarized membrane delivery via the Golgi apparatus is important for neuronal morphogenesis during brain development (8–10, 21), but whether impairment of this process can cause neuronal death with consequent neurological impairment in vivo is currently unknown.

Members of the golgin family of coiled-coil proteins are required for maintenance of Golgi organization and are important for the specificity and efficiency of membrane traffic at the Golgi apparatus (22, 23). One of the best-studied golgins, GM130 (also known as GOLGA2), contributes to Golgi ribbon morphology and can tether transport vesicles to facilitate endoplasmic reticulum (ER) to Golgi traffic (24–27). It has also been implicated in Golgi positioning and cytoskeletal regulation (4, 28) and can contribute to the organization of neuronal Golgi outposts, at least in *Drosophila* (13). However, the physiological importance and in vivo functions of GM130 have yet to be explored in a mammal.

Here, we generated GM130 knockout (KO) mice and investigated the consequences of GM130 loss upon Golgi architecture and function within the nervous system. We find that loss of GM130 leads to disrupted organization and altered positioning of the Golgi apparatus in cerebellar Purkinje cells, which is accompanied by impaired polarized trafficking to the apical dendrite. Importantly, we find that these cellular defects manifest as a loss of Purkinje cell viability and progressive cerebellar atrophy, leading to ataxia. Our findings therefore indicate that disruption

Significance

It has been known for many years that the Golgi apparatus, the central organelle of the secretory pathway, is fragmented upon neurodegenerative disease. However, it has remained an open question whether Golgi disruption contributes to neuronal death, as seen in disease, or is simply a consequence of this process. Here, we show that knocking out the Golgi protein GM130 in mice causes Golgi fragmentation and impaired secretory trafficking in Purkinje neurons, resulting in cell death and ataxia. The cell death and ataxia are first observed in postnatal development, but worsen with age. These findings indicate that targeted disruption of the Golgi apparatus can result in neuronal loss in vivo, supporting the view that Golgi dysfunction can contribute to neurodegeneration.

Author contributions: C.L., M.M., P.R., F.G., M.L., and S.B. designed research; C.L., M.M., Q.L., P.R., Q.P., and Z.Y. performed research; C.L., M.M., Q.L., P.R., Q.P., Z.Y., and S.B. analyzed data; and M.L. and S.B. wrote the paper.

The authors declare no conflict of interest.

This article is a PNAS Direct Submission.

Freely available online through the PNAS open access option.

[1]C.L., M.M., and Q.L. contributed equally to this work.

[2]To whom correspondence may be addressed. Email: slbao@genetics.ac.cn or martin.lowe@manchester.ac.uk.

This article contains supporting information online at www.pnas.org/lookup/suppl/doi:10.1073/pnas.1608576114/-/DCSupplemental.

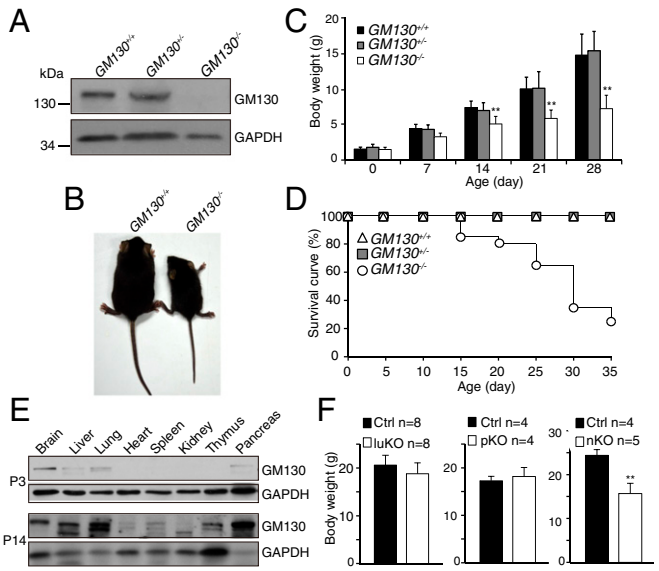

Fig. 1. GM130 is critical for growth and survival of mice. (*A*) Absence of GM130 protein in *GM130*$^{-/-}$ mice. (*B*) Representative image of WT and *GM130*$^{-/-}$ littermates. (*C*) Body weight histogram of *GM130*$^{+/+}$ (n = 20), *GM130*$^{+/-}$ (n = 41), and *GM130*$^{-/-}$ (n = 21) mice. $^{**}P < 0.01$. (*D*) Survival curve of *GM130*$^{+/+}$, *GM130*$^{+/-}$, and *GM130*$^{-/-}$ mice. (*E*) Expression pattern of GM130 in P3 and P14 mice. (*F*) Body weight of pancreas (p)-, lung (lu)-, and neural (n)-specific KO mice compared with WT (Ctrl) littermates at 8–9 wk of age. $^{**}P < 0.01$.

of the Golgi apparatus and impairment of secretory trafficking result in neuronal loss in vivo and thus may contribute to the phenotypes observed in neurodevelopmental and neurodegenerative disease.

Results

Generation of GM130 KO Mice. To determine the physiological importance of GM130 in vivo, we generated a global KO mouse (*GM130*$^{-/-}$) by homologous recombination (Fig. S1). The *GM130*$^{-/-}$ mice, which lacked detectable GM130 (Fig. 1*A*), were born at a normal Mendelian ratio, indicating GM130 is not essential for embryonic development. However, deletion of GM130 resulted in reduced growth (Fig. 1 *B* and *C*) and death before postnatal day 35 (P35) (Fig. 1*D*).

To explore how loss of GM130 causes growth retardation and death, the temporal expression of GM130 in different mouse organs was examined. We found that GM130 is highly expressed in the brain of newborn mice (P3), and although widely expressed, it is particularly abundant in liver, pancreas, and lung during postnatal development (P14) (Fig. 1*E*). To determine how organ-specific loss of GM130 affects postnatal development, we generated conditional KO mice in which GM130 was selectively knocked out in brain, pancreas, or lung (Fig. S2). Postnatal development and survival of mice were not affected in mice lacking GM130 in either the pancreas or lung (Fig. 1*F*), although GM130 was highly expressed in these organs. However, when GM130 was deleted in the brain by crossing *GM130*$^{fl/fl}$ with mice bearing a *Nestin-Cre* transgene, which is expressed throughout the nervous system (29), the neuron-specific KO offspring (*GM130*-nKO mice) showed significant growth retardation (Fig. 1*F*). This result indicates that GM130 expression in the brain is required for normal growth in mice. The *GM130*-nKO mice were able to breed and did not show reduced survival relative to *GM130*$^{fl/fl}$ [control mice (Ctrl)] littermates up to 1.5 y of age. The growth retardation observed in *GM130*-nKO mice was less than that in *GM130*$^{-/-}$ mice, suggesting that GM130 has functions in cell types beyond those in which *Nestin-Cre* is active.

Motor Defects in GM130 KO Mice. The *GM130*$^{-/-}$ mice displayed a striking ataxia phenotype (Movie S1 and Fig. S3*A*). The mice staggered and could not stand steady on their hind legs, indicating GM130 is required for proper motor control during postnatal development. Consistent with the ataxia phenotype seen in *GM130*$^{-/-}$ mice, *GM130*-nKO mice also displayed motor coordination defects (Movie S2). These were mild in young animals but progressively worsened with age (Movie S3), and tremor was obvious. The *GM130*-nKO mice also displayed a limp reflex when lifted by their tail (Fig. 2*A*), consistent with a neurodegenerative defect (30). A footprint assay revealed an ataxic walking gait and diminished stride (Fig. 2 *B* and *C*). In contrast, both *Nestin-Cre* transgenic mice and *GM130*$^{fl/fl}$ mice did not display any motor abnormalities. To assess motor coordination quantitatively, the *GM130*-nKO mice and control littermates were subjected to rotarod testing. In multiple trails, *GM130*-nKO mice showed a slight reduction in time spent on the rotarod at 3 wk of age (Fig. 2*D*), which was much more profound at 8 and 12 wk of age (Fig. 2*E* and Fig. S3 *B*–*D*). *GM130*-nKO mice also needed a longer time to cross balance beams of multiple sizes (Fig. 2 *F* and *G*). Together, these results indicate that deletion of GM130 in the central nervous system leads to severe neurological dysfunction.

Progressive Cerebellar Atrophy and Purkinje Cell Loss in *GM130*-nKO Mice. To reveal the basis of the motor phenotype of *GM130*-nKO mice, adult brains from *GM130*$^{fl/fl}$ and *GM130*-nKO mice were analyzed. No gross changes in brain architecture were observed in the forebrain or midbrain of *GM130*-nKO mice; however, the cerebellar size was dramatically reduced (Fig. 3 *A* and *B*).

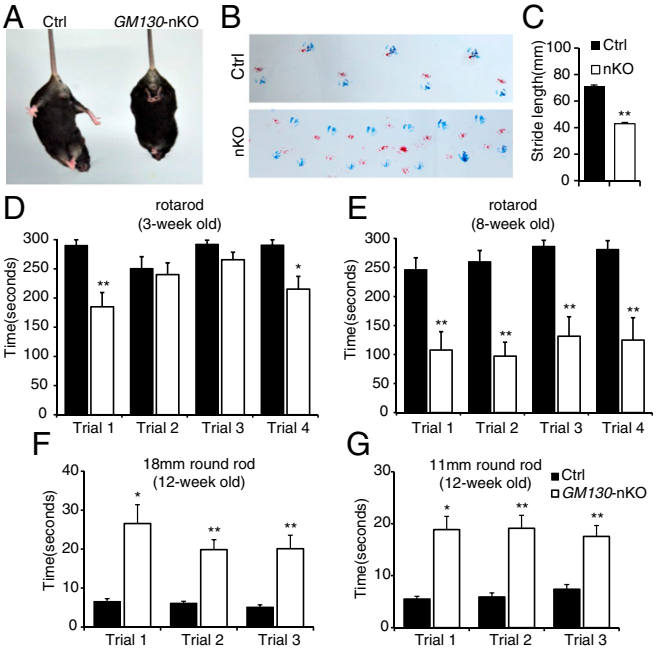

Fig. 2. Motor disorders of *GM130*-nKO mice. (*A*) Limb clasping reflex in *GM130*-nKO mouse. (*B*) Gait of mice was assessed with footprint assay. Footprints in red and blue indicate those made by forepaws and hind paws, respectively. (*C*) Shorter stride lengths of *GM130*-nKO mice (n = 5, $^{**}P < 0.01$). (*D* and *E*) Time spent on a rotarod for control and *GM130*-nKO mice at age 3-wk (*D*) and 8-wk (*E*). n = 7 control mice, n = 8 *GM130*-nKO mice; $^{*}P < 0.05$, $^{**}P < 0.01$. Results from four independent trials are shown. Data are presented as the mean ± SEM. (*F* and *G*) Time needed to traverse an 18-mm (*F*) and 11-mm (*G*) round wooden rod. n = 9 control mice, n = 9 *GM130*-nKO mice; $^{*}P < 0.05$, $^{**}P < 0.01$. Results from three independent trials are shown. Data are presented as the mean ± SEM.

Therefore, we focused our attention on the cerebellum. Histological analysis by Nissl staining revealed a dramatic loss of Purkinje cells in adult *GM130*-nKO cerebellum (Fig. 3*C*). By comparing the cerebellum at different ages, we found that loss of Purkinje cells, marked by antibodies to calbindin-D28K, began in the third postnatal week, most noticeably from lobules X and IX (Fig. 3 *D–F*), with Purkinje cell degeneration occurring in other regions as the mice became older (Fig. S4 *A–C*). In contrast to Purkinje cells, there was no degeneration of neurons within the molecular or granule layers of the cerebellum (Fig. S4*D*). The results indicate a progressive cerebellar atrophy and degeneration of Purkinje cells in the *GM130*-nKO mice, as opposed to a neurogenesis defect occurring early in development. The progressive degeneration of Purkinje cells correlated with impaired motor function, which was also progressive in nature (Fig. 2 and Fig. S3 *B–D*). The loss of Purkinje cells in the *GM130*-nKO mice also correlated with a significant decrease in the thickness of the molecular layer (Fig. 3*F*) and increased staining of the astrocyte marker GFAP, consistent with neuronal damage, in cerebellar regions where Purkinje cell loss occurred (Fig. 3*G*). Staining for the apoptosis marker cleaved caspase 3 indicated that there was significant apoptotic cell death of Purkinje neurons in the *GM130*-nKO mice (Fig. S5 *A* and *B*). Consistent with the Purkinje cell loss observed in the *GM130*-nKO mice, the global deletion of GM130 also resulted in dramatically reduced numbers of Purkinje cells (Fig. S5*C*).

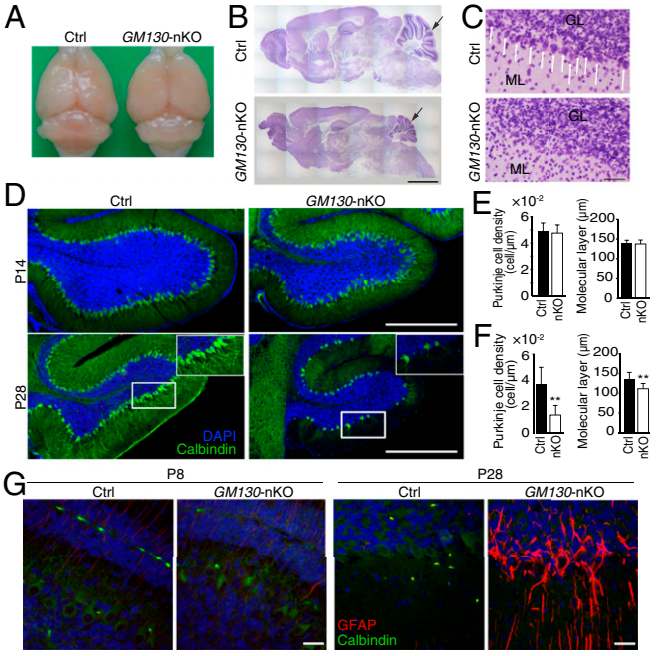

Fig. 3. Age-dependent cerebellar atrophy in *GM130*-nKO mice. (*A*) Gross morphology of brains from adult control and *GM130*-nKO mice. (*B* and *C*) Nissl staining of sagittal sections of brain (*B*) and cerebellum (*C*) from 7-mo-old control and *GM130*-nKO mice. Black arrows in *B* indicate the position of the cerebellum. (Scale bar in *B*, 500 μm.) White arrows in *C* indicate Purkinje cells. The granule cell layer (GL) and molecular layer (ML) are indicated. (Scale bar in *C*, 50 μm.) (*D*) Purkinje cells (labeled with calbindin-D28K, green) in lobule X of the cerebellum of *GM130*-nKO and littermate control mice at age 2 wk (*Upper*) and 4 wk (*Lower*). Nuclei are stained with DAPI (blue). (Scale bar, 500 μm.) (*E* and *F*) Quantification of the Purkinje cell density and molecular layer thickness in lobules X and IX of *GM130*-nKO and littermate control mice at age 2 wk (*E*) and 4 wk (*F*). $n = 3$; $^{**}P < 0.01$. Data are presented as the mean ± SD. (*G*) Immunohistochemical staining of the astrocyte marker glial fibrillary acidic protein (GFAP, red) and calbindin-D28K (green) in the cerebellum of control and *GM130*-nKO mice. (Scale bar, 20 μm.)

Disruption of Golgi Architecture and Positioning upon GM130 KO. Studies in cultured cells have revealed a role for GM130 in maintaining mammalian Golgi ribbon organization and pericentrosomal positioning (25, 31). GM130 also participates in vesicle tethering during ER-to-Golgi traffic (24, 26, 27), and can function as a scaffold for activation of Cdc42 or Stk25 that is relevant for cell migration (32–34). To elucidate the cellular basis of the ataxic phenotype and Purkinje cell degeneration of *GM130*-nKO mice, we used antibodies to golgin-84 and TGN38, markers of the *cis* and *trans*-Golgi respectively, to analyze Golgi structure in Purkinje cells from mice at ages of P8, P14 and P28 by immunostaining. Purkinje cells from control mice at all ages had an elaborate Golgi ribbon, with Golgi elements extending around the nucleus of the cell soma, whereas loss of GM130 resulted in a compaction of the Golgi apparatus at P14 and P28 (Fig. 4 *A* and *B* and see Fig. S8). Changes in Golgi ultrastructure in the Purkinje cells were clearly observed using transmission electron microscopy with a loss of cisternal stacking and cisternal length and an accumulation of vesicular profiles localized to the perinuclear region (Fig. 4 *C* and *D*). These results are consistent with our observations in *GM130*$^{-/-}$ mouse embryonic fibroblast (MEF) cells (Fig. S6). A similar disruption of Golgi architecture was seen in granule cells within the cerebellum of the *GM130*-nKO mice, and also in nonneuronal cell types in the *GM130*$^{-/-}$ mice, indicating that GM130 is important for maintaining Golgi organization in many cell types in vivo (Fig. S7).

In WT mice at P8 we observed Golgi outposts in primary dendrites of Purkinje cells, as expected from other studies (8–10, 21). The outposts were absent from Purkinje cells lacking GM130, which is consistent with results in *Drosophila* (13). Interestingly, Golgi outposts were not observed in Purkinje cell dendrites at P14 and P28, even in WT mice (Fig. 4*A*), suggesting that the Golgi apparatus undergoes dynamic changes in its dendritic localization during neuronal development.

Importantly, we found that loss of GM130 altered the position of the Golgi apparatus in the soma of Purkinje cells. In control mice, although the Golgi ribbon extended around the nucleus, it was enriched at the apical pole and extended to the initial segment of the primary dendrite, close to the molecular layer (Fig. 4 *A*, *B*, and *E*). In contrast, the Golgi was predominantly found at the opposite side of the soma to the primary dendrite in *GM130*-nKO mice at P14 and P28, indicating a loss of apical polarity of the Golgi apparatus (Fig. 4 *A*, *B*, and *E*). This finding is consistent with the loss of Golgi polarity seen upon shRNA-mediated depletion of GM130 from hippocampal granule cells (10). The pericentrosomal positioning of the mammalian Golgi apparatus helps determine its polarized distribution in various cell types (7). To determine whether loss of GM130 results in altered association of the Golgi with the centrosome in Purkinje cells, Golgi and centrosome positioning were analyzed in parallel. As shown in Fig. 4*F*, in control mice the Golgi apparatus was closely associated with the Purkinje cell centrosome, labeled with γ-tubulin, which was located apically near the base of the primary dendrite. In *GM130*-nKO mice, the centrosome retained its apical polarity, but the Golgi apparatus was completely dissociated from it (Fig. 4*F*). A likely explanation for this effect is the loss of GM130 binding protein A kinase anchoring protein of 450 kDa (AKAP450), which helps link the Golgi apparatus to the centrosome (35), from the Golgi in the *GM130*-nKO Purkinje neurons (Fig. S8*A*). In contrast, the Golgi association of Stk25, which has been implicated in Golgi polarity (32), was retained in the absence of GM130 (Fig. S8*B*). Together these results indicate that although GM130 is not required for initial Golgi polarization, it is essential to maintain the polarized distribution of the Golgi apparatus in Purkinje cells, most likely through its association with AKAP450 and the centrosome.

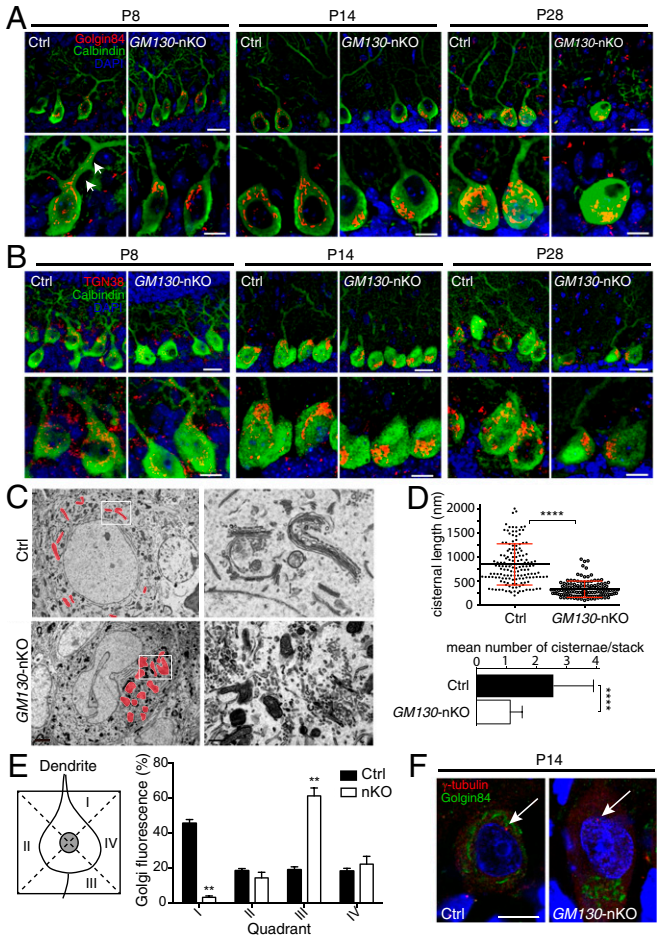

Fig. 4. Altered Golgi morphology and positioning in *GM130*-nKO mice. (*A* and *B*) Golgin-84 (*A*) or TGN38 (*B*) immunohistochemical staining (red) of *cis*- or *trans*-Golgi and calbindin-D28K (green) of Purkinje cells in mice at different ages. White arrows in *A* indicate Golgi elements within the primary dendrite. (Scale bar, *Upper* 20 μm and *Lower* 10 μm.) (*C*) Electron micrographs of the Golgi apparatus in Purkinje cells of control and *GM130*-nKO mice at P30. The pink shading shows the location of Golgi membranes. (Scale bar, *Left* 2 μm and *Right* 0.5 μm.) (*D*) Quantitation of Golgi morphology for cisternal length (*Top*, $n = 153$ for Ctrl and 124 for GM130-nKO, n = number of Golgi cisternae counted) and mean number of cisternae per stack from Purkinje cells of control and *GM130*-nKO mice at P28 (*Bottom*, $n = 50$ for Ctrl and 104 for GM130-nKO, where n = number of Golgi stacks counted). Results are expressed as mean ± SD ****$P < 0.0001$. (*E*) Quantitation of Golgi positioning in Purkinje cells of control and *GM130*-nKO mice at P14. The scheme used to determine Golgi distribution in Purkinje cells is shown at *Left* with quantitation shown at *Right*. The Golgi distribution was assessed using Golgin-84 as the marker and expressed as the average percentage of total cellular fluorescence in each of the four quadrants, calculated for each cell before averaging. $n = 23$–30; **$P < 0.01$. Data are presented as mean ± SEM. (*F*) Immunofluorescence of Purkinje cells for Golgin-84 (green) and the centrosome marker γ-tubulin (red) in control and *GM130*-nKO mice. White arrows indicate the centrosome. (Scale bar, 10 μm.)

Deficient Secretory Cargo Trafficking upon GM130 KO. The polarized distribution of the Golgi apparatus in neuronal cells is required for directed trafficking of secretory cargos into the dendrite, which is important for dendritic growth during development (8–10, 21). GM130 participates in ER-to-Golgi traffic (24, 26), functioning as a tether for ER-derived transport vesicles (27). Secretory trafficking was therefore analyzed in GM130 KO cells, using the model cargo vesicular stomatitis virus G protein (VSVG) fused to GFP. In both cultured primary MEFs and cerebellar neurons, deletion of GM130 led to a reduced rate of trafficking of VSVG–GFP from the ER to the Golgi apparatus (Fig. 5 *A* and *B* and Fig. S9), indicating a role for GM130 in this trafficking step in these cells. We then analyzed the morphology of dendrites in Purkinje cells of the KO mice. In WT mice, an elaborate dendritic tree was obvious at P9, and by P30 there was a dramatic expansion of dendritic arbors, as expected (Fig. 5*C*). Dendritic morphology was relatively normal at P9 in *GM130*-nKO mice (Fig. 5*C*), indicating that GM130 is dispensable for initiation of dendrite formation and initial growth of the dendritic tree. However, strikingly, there was a dramatic reduction both in dendritic size and arborization in *GM130*-nKO Purkinje cells at P30 compared with WT (Fig. 5*C*). Indeed the dendrite was smaller than that seen at P9, indicating not only a failure to expand but also significant amount of dendritic atrophy. Together these results indicate impaired secretion and defective dendritic maintenance upon loss of GM130.

To further assess secretory trafficking in the cerebellum of *GM130*-nKO mice, we focused on synaptic receptors that have to transit the Golgi apparatus on their way to the neuronal plasma membrane, where they function in neurotransmission (36, 37). Levels of plasma membrane AMPA-type glutamate receptor subunits were assessed by blotting the postsynaptic density (PSD) fraction isolated from the cerebellum of *GM130*-nKO mice. There were decreased amounts of both GluR1 and GluR2 in the PSD fraction of the *GM130*-nKO mice compared with control, even though total abundance was not affected (Fig. 5 *D* and *E*), consistent

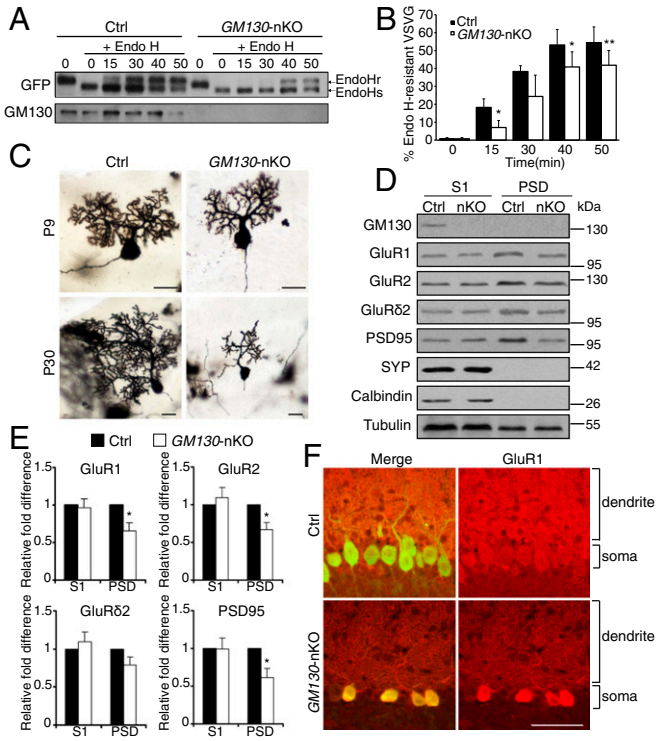

Fig. 5. Impaired secretory trafficking after loss of GM130. (*A*) Effect of loss of GM130 on VSVG–GFP trafficking in cultured cerebellar neurons at DIV14 (14 days in vitro) from control and *GM130*-nKO mice. (*B*) The levels of Endo H-sensitive and -resistant forms of VSVG–GFP were quantified and the percentage of Endo H-resistant form with respect to total VSVG–GFP was calculated. $n = 4$. Data are presented as mean ± SD. (*C*) Golgi staining of Purkinje cells. (Scale bar, 20 μm.) (*D*) Cerebella from control and *GM130*-nKO mice at P16 were lysed and fractionated for immunoblotting of postnuclear supernatant (S1) and PSD fractions with the indicated antibodies. Equal protein was loaded for each fraction. (*E*) Quantification of protein abundance in the homogenate (S1) and PSD fractions. $n = 4$; *$P < 0.05$, **$P < 0.01$. (*F*) Immunohistochemical staining for GluR1 (red) and calbindin-D28K (green) of Purkinje cells in control and *GM130*-nKO mice. (Scale bar, 50 μm.) The Purkinje cell soma and dendritic areas are indicated.

CELL BIOLOGY

with impaired secretory traffic to the synaptic membrane. In support of this conclusion, we found soma to dendritic trafficking of GluR1 was reduced in *GM130*-nKO Purkinje neurons (Fig. 5*F*). It has been reported that decreased abundance of the GluR2 subunit can lead to high Ca^{2+} influx (38), which can result in Purkinje cell death. There was also reduced PSD95, which scaffolds several types of neurotransmitter receptors including NMDA and AMPA-type glutamate receptors at the postsynaptic membrane (39), in the PSD fraction (Fig. 5 *D* and *E*). Reduced PSD95 can cause reduced AMPA receptor abundance at the synapse and longer NMDA-mediated long-term potentiation (40). Thus, defective neurotransmission as a consequence of reduced neurotransmitter receptor abundance and stability at the synapse is likely to contribute to impaired functionality and long-term survival of Purkinje cells in the cerebellum of *GM130*-nKO mice.

Analysis of Golgins and GRASP65 in the Cerebellum. Given the particular sensitivity of Purkinje neurons to loss of GM130, it was of interest to assess relative levels of GM130 and related golgins, in different neuronal types, both in control and *GM130*-nKO mice. As shown in Fig. S8*C*, GM130 is expressed in Purkinje cells and in neurons within the granule and molecular layers of control cells. The staining for GM130 was stronger in Purkinje cells, reflecting the increased abundance of Golgi membranes in this cell type. The same was true for two other golgins, golgin-84 and TMF1, which are localized to the *cis*-Golgi and *trans*-Golgi, respectively (Fig. 4*A* and Fig. S8*D*). Similarly, staining for the *cis*-Golgi golgin Golgi microtubule-associated protein of 210 kDa (GMAP210), which, like GM130, also functions in ER-to-Golgi transport (27, 41), was strong in Purkinje neurons, although harder to detect in other neuronal types present within the cerebellum (Fig. S8*E*). In *GM130*-nKO mice, the levels of the golgins studied were unaffected (Fig. 4*A* and Fig. S8*D*), although there was a slight reduction in abundance of GMAP210 (Fig. S8*E*). Golgi reassembly and stacking protein of 65 kDa (GRASP65), which is anchored to the Golgi membrane via association with GM130 (25, 42), was present in Purkinje cells and other neuronal types within the cerebellum of control mice. In *GM130*-nKO mice, it was lost from the Golgi, as expected (Fig. S8*F*). Together these results suggest that the particular sensitivity of Purkinje cells to loss of GM130 is not due to a deficit in expression of other golgins or GRASP65 in this cell type.

Discussion

In this study we report that targeted KO of the golgin GM130 in mice leads to degeneration of Purkinje neurons within the cerebellum. Within Purkinje neurons, GM130 is required for Golgi positioning via association with the centrosome, and for efficient ER-to-Golgi trafficking (Fig. S10). Both processes are required for polarized delivery of secretory cargo to the dendrite, which is required for growth and maintenance of the dendritic tree. Loss of GM130 leads to dendrite atrophy, Purkinje cell degeneration, and generation of an ataxic phenotype in mice.

Previous work has shown that the polarized distribution of the Golgi apparatus is required for dendritic initiation from the soma and subsequent growth, a process that requires the delivery of large amounts of newly synthesized plasma membrane components via the secretory pathway (8, 21). Knockout of GM130 did not affect initiation or early growth of the Purkinje cell dendrite, but was required for maintenance of the dendritic tree. This finding suggests there is a higher requirement for directed secretory traffic for the expansion and maintenance of the dendritic tree, as opposed to its initial formation, at least in Purkinje cells. GM130 impairs membrane delivery into the apical dendrite in two ways: loss of Golgi positioning and lower rates of ER-to-Golgi traffic, most likely due to defects in vesicle tethering.

A recent study reported that RNAi-mediated depletion of GM130 in hippocampal neurons results in mild impairment of dendritic initiation (10). In contrast, we find that in Purkinje neurons, dendritic initiation still occurs in the absence of GM130. Notably, we find that Purkinje neurons are particularly susceptible to loss of GM130 in vivo. The reason for this is currently unclear. A possible explanation is redundancy in golgin function, which may vary between different types of neurons (22, 23). However, the abundant Purkinje cell expression of other *cis*-Golgi golgins that could in theory compensate for loss of GM130 argues against this possibility. Rather, we favor the hypothesis that Purkinje cells are particularly susceptible to perturbations of secretory traffic due to their extremely large dendritic tree, which requires a significant input of material for both its growth and its maintenance. The relatively large amounts of Golgi in Purkinje cells would be consistent with this idea. Interestingly, knockout of the GM130 binding partner GRASP65 in mice fails to elicit a phenotype (43). This has been attributed to compensation by the related protein GRASP55 (43), which does not interact with GM130 in vivo (44). Thus, even though loss of GM130 resulted in a failure to recruit GRASP65 to the Golgi, the phenotypes we observe are likely independent of GRASP65.

Cell-culture–based studies have implicated GM130 in a number of cellular processes in addition to secretory trafficking, including cytoskeletal regulation, which is important for cell migration and cell division (4, 31, 33, 34). It was therefore surprising that the GM130 KO mice did not display any overt developmental phenotype; pups were born at normal weight and looked morphologically normal. These findings would appear inconsistent with a major role for GM130 in cell migration or cell division in vivo, processes that are particularly important during embryonic development. However, an alternative explanation is that GM130 function in these processes is redundant, possibly with another golgin, or that the developing animal can compensate for loss of GM130 in a way not possible in cultured cells. Further studies will be required to discriminate between these possibilities. Interestingly, a human patient with a loss-of-function GM130 mutation has recently been described (45). This patient lacked any neonatal phenotype, but developed neuromuscular defects in the first year of life. Hence, in humans, it would seem GM130 is also dispensable during embryonic development. It would also appear that an important role for GM130 in the nervous system is conserved between mice and humans.

How similar the neuronal degeneration we observe upon GM130 KO is to that observed in progressive neurodegenerative disease is currently unclear. The loss of Purkinje cells in the GM130 KO mice starts around 3 wk into postnatal development and progressively worsens as the mice age. The most common neurodegenerative diseases typically manifest only later in life, although the spinocerebellar ataxias, in which Purkinje cell death is commonly observed, can appear much earlier in life (46). The cellular phenotypes we observe in the GM130 KO mice could be considered neurodevelopmental. Although Purkinje neurons are born and specified before the time when phenotypes start to manifest, in mice they continue to develop their dendritic tree for up to 3 wk following birth (47, 48). Hence, a failure of Purkinje cells to properly grow or maintain the dendritic tree during the first weeks of postnatal development could explain the neurological defects we observe. This is different from an inability to maintain a fully formed dendritic network, as occurs when mature neurons undergo degeneration in later onset disease. Nevertheless, the demonstration that Golgi dysfunction causes neuronal loss in vivo, combined with the observation that neuronal loss and ataxia worsen with age upon loss of GM130, indicates that this process could, in principle, result in or at least contribute to the neurodegeneration that occurs in human disease. In support of this possibility, it has been shown that α-synuclein can perturb ER-to-Golgi traffic in Parkinson's disease models (49), and that the Aβ-fragment of APP that causes Alzheimer's disease, and the pathogenic form of ataxin-2 that causes SCA2, both disrupt Golgi organization (19, 50). Hence, Golgi dysfunction and defective

secretory trafficking, which could be attributable to a number of primary causes, may represent a significant pathogenic mechanism of neurodegenerative disease in humans.

Materials and Methods

All animal experiments were approved by the animal welfare committees of Institute of Genetics and Developmental Biology. Detailed methods for KO mouse generation and phenotypic analysis, immunohistochemistry, and EM and biochemical fractionation and trafficking experiments can be found in the *SI Materials and Methods*. This section also contains details of relevant antibodies used in this study and the methods used for quantitative analysis of data.

ACKNOWLEDGMENTS. We thank Peizhun Zhang and Yaqing Wang for their input in these studies; Philip Woodman, Viki Allan, Stephen High, and Hugh Piggins for their comments on the manuscript; and Samantha Forbes of the University of Manchester Faculty of Biology, Medicine and Health EM core facility for help with the EM. This work was supported by the National Natural Sciences Foundation of China (Grants 31571379 and 31371378) and the Biotechnology and Biological Sciences Research Council (Grant BB/I007717/1 and Partnering Award BB/H531600/1).

1. Farquhar MG, Palade GE (1998) The Golgi apparatus: 100 years of progress and controversy. *Trends Cell Biol* 8(1):2–10.
2. Colanzi A, Corda D (2007) Mitosis controls the Golgi and the Golgi controls mitosis. *Curr Opin Cell Biol* 19(4):386–393.
3. Sanders AA, Kaverina I (2015) Nucleation and dynamics of Golgi-derived microtubules. *Front Neurosci* 9:431.
4. Wei JH, Zhang ZC, Wynn RM, Seemann J (2015) GM130 regulates Golgi-derived spindle assembly by activating TPX2 and capturing microtubules. *Cell* 162(2):287–299.
5. Klumperman J (2011) Architecture of the mammalian Golgi. *Cold Spring Harb Perspect Biol* 3(7):a005181.
6. Lowe M (2011) Structural organization of the Golgi apparatus. *Curr Opin Cell Biol* 23(1):85–93.
7. Yadav S, Linstedt AD (2011) Golgi positioning. *Cold Spring Harb Perspect Biol* 3(5):a005322.
8. Horton AC, et al. (2005) Polarized secretory trafficking directs cargo for asymmetric dendrite growth and morphogenesis. *Neuron* 48(5):757–771.
9. Matsuki T, et al. (2010) Reelin and stk25 have opposing roles in neuronal polarization and dendritic Golgi deployment. *Cell* 143(5):826–836.
10. Huang W, et al. (2014) Protein kinase LKB1 regulates polarized dendrite formation of adult hippocampal newborn neurons. *Proc Natl Acad Sci USA* 111(1):469–474.
11. Horton AC, Ehlers MD (2004) Secretory trafficking in neuronal dendrites. *Nat Cell Biol* 6(7):585–591.
12. Ori-McKenney KM, Jan LY, Jan YN (2012) Golgi outposts shape dendrite morphology by functioning as sites of acentrosomal microtubule nucleation in neurons. *Neuron* 76(5):921–930.
13. Zhou W, et al. (2014) GM130 is required for compartmental organization of dendritic golgi outposts. *Curr Biol* 24(11):1227–1233.
14. Valenzuela JI, Perez F (2015) Diversifying the secretory routes in neurons. *Front Neurosci* 9:358.
15. Gonatas NK, et al. (1992) Fragmentation of the Golgi apparatus of motor neurons in amyotrophic lateral sclerosis. *Am J Pathol* 140(3):731–737.
16. Mourelatos Z, Gonatas NK, Stieber A, Gurney ME, Dal Canto MC (1996) The Golgi apparatus of spinal cord motor neurons in transgenic mice expressing mutant Cu,Zn superoxide dismutase becomes fragmented in early, preclinical stages of the disease. *Proc Natl Acad Sci USA* 93(11):5472–5477.
17. Stieber A, Mourelatos Z, Gonatas NK (1996) In Alzheimer's disease the Golgi apparatus of a population of neurons without neurofibrillary tangles is fragmented and atrophic. *Am J Pathol* 148(2):415–426.
18. Mizuno Y, et al. (2001) Familial Parkinson's disease. Alpha-synuclein and parkin. *Adv Neurol* 86:13–21.
19. Huynh DP, Yang HT, Vakharia H, Nguyen D, Pulst SM (2003) Expansion of the polyQ repeat in ataxin-2 alters its Golgi localization, disrupts the Golgi complex and causes cell death. *Hum Mol Genet* 12(13):1485–1496.
20. Rabouille C, Haase G (2016) Editorial: Golgi pathology in neurodegenerative diseases. *Front Neurosci* 9:489.
21. Ye B, et al. (2007) Growing dendrites and axons differ in their reliance on the secretory pathway. *Cell* 130(4):717–729.
22. Witkos TM, Lowe M (2016) The Golgin family of coiled-coil tethering proteins. *Front Cell Dev Biol* 3:86.
23. Gillingham AK, Munro S (2016) Finding the Golgi: Golgin coiled-coil proteins show the way. *Trends Cell Biol* 26(6):399–408.
24. Seemann J, Jokitalo EJ, Warren G (2000) The role of the tethering proteins p115 and GM130 in transport through the Golgi apparatus in vivo. *Mol Biol Cell* 11(2):635–645.
25. Puthenveedu MA, Bachert C, Puri S, Lanni F, Linstedt AD (2006) GM130 and GRASP65-dependent lateral cisternal fusion allows uniform Golgi-enzyme distribution. *Nat Cell Biol* 8(3):238–248.
26. Marra P, et al. (2007) The biogenesis of the Golgi ribbon: The roles of membrane input from the ER and of GM130. *Mol Biol Cell* 18(5):1595–1608.
27. Wong M, Munro S (2014) Membrane trafficking. The specificity of vesicle traffic to the Golgi is encoded in the golgin coiled-coil proteins. *Science* 346(6209):1256898.
28. Nakamura N (2010) Emerging new roles of GM130, a cis-Golgi matrix protein, in higher order cell functions. *J Pharmacol Sci* 112(3):255–264.
29. Tronche F, et al. (1999) Disruption of the glucocorticoid receptor gene in the nervous system results in reduced anxiety. *Nat Genet* 23(1):99–103.
30. Côté F, Collard JF, Julien JP (1993) Progressive neuronopathy in transgenic mice expressing the human neurofilament heavy gene: A mouse model of amyotrophic lateral sclerosis. *Cell* 73(1):35–46.
31. Rivero S, Cardenas J, Bornens M, Rios RM (2009) Microtubule nucleation at the cis-side of the Golgi apparatus requires AKAP450 and GM130. *EMBO J* 28(8):1016–1028.
32. Preisinger C, et al. (2004) YSK1 is activated by the Golgi matrix protein GM130 and plays a role in cell migration through its substrate 14-3-3zeta. *J Cell Biol* 164(7):1009–1020.
33. Kodani A, Kristensen I, Huang L, Sütterlin C (2009) GM130-dependent control of Cdc42 activity at the Golgi regulates centrosome organization. *Mol Biol Cell* 20(4):1192–1200.
34. Baschieri F, et al. (2014) Spatial control of Cdc42 signalling by a GM130-RasGRF complex regulates polarity and tumorigenesis. *Nat Commun* 5:4839.
35. Hurtado L, et al. (2011) Disconnecting the Golgi ribbon from the centrosome prevents directional cell migration and ciliogenesis. *J Cell Biol* 193(5):917–933.
36. Bredt DS, Nicoll RA (2003) AMPA receptor trafficking at excitatory synapses. *Neuron* 40(2):361–379.
37. Lau CG, Zukin RS (2007) NMDA receptor trafficking in synaptic plasticity and neuropsychiatric disorders. *Nat Rev Neurosci* 8(6):413–426.
38. Carriedo SG, Yin HZ, Sensi SL, Weiss JH (1998) Rapid Ca2+ entry through Ca2+-permeable AMPA/Kainate channels triggers marked intracellular Ca2+ rises and consequent oxygen radical production. *J Neurosci* 18(19):7727–7738.
39. Kim E, Sheng M (2004) PDZ domain proteins of synapses. *Nat Rev Neurosci* 5(10):771–781.
40. Béïque JC, et al. (2006) Synapse-specific regulation of AMPA receptor function by PSD-95. *Proc Natl Acad Sci USA* 103(51):19535–19540.
41. Roboti P, Sato K, Lowe M (2015) The golgin GMAP-210 is required for efficient membrane trafficking in the early secretory pathway. *J Cell Sci* 128(8):1595–1606.
42. Barr FA, Puype M, Vandekerckhove J, Warren G (1997) GRASP65, a protein involved in the stacking of Golgi cisternae. *Cell* 91(2):253–262.
43. Veenendaal T, et al. (2014) GRASP65 controls the cis Golgi integrity in vivo. *Biol Open* 3(6):431–443.
44. Shorter J, et al. (1999) GRASP55, a second mammalian GRASP protein involved in the stacking of Golgi cisternae in a cell-free system. *EMBO J* 18(18):4949–4960.
45. Shamseldin HE, Bennett AH, Alfadhel M, Gupta V, Alkuraya FS (2016) GOLGA2, encoding a master regulator of golgi apparatus, is mutated in a patient with a neuromuscular disorder. *Hum Genet* 135(2):245–251.
46. Paulson HL (2009) The spinocerebellar ataxias. *J Neuroophthalmol* 29(3):227–237.
47. Weiss GM, Pysh JJ (1978) Evidence for loss of Purkinje cell dendrites during late development: A morphometric Golgi analysis in the mouse. *Brain Res* 154(2):219–230.
48. Sotelo C, Dusart I (2009) Intrinsic versus extrinsic determinants during the development of Purkinje cell dendrites. *Neuroscience* 162(3):589–600.
49. Cooper AA, et al. (2006) Alpha-synuclein blocks ER-Golgi traffic and Rab1 rescues neuron loss in Parkinson's models. *Science* 313(5785):324–328.
50. Joshi G, Chi Y, Huang Z, Wang Y (2014) Aβ-induced Golgi fragmentation in Alzheimer's disease enhances Aβ production. *Proc Natl Acad Sci USA* 111(13):E1230–E1239.
51. Sato K, Roboti P, Mironov AA, Lowe M (2015) Coupling of vesicle tethering and Rab binding is required for in vivo functionality of the golgin GMAP-210. *Mol Biol Cell* 26(3):537–553.
52. Roboti P, Witkos TM, Lowe M (2013) Biochemical analysis of secretory trafficking in mammalian cells. *Methods Cell Biol* 118:85–103.
53. Zhou Z, et al. (2010) PRMT5 regulates Golgi apparatus structure through methylation of the golgin GM130. *Cell Res* 20(9):1023–1033.
54. Carlin RK, Grab DJ, Cohen RS, Siekevitz P (1980) Isolation and characterization of postsynaptic densities from various brain regions: Enrichment of different types of postsynaptic densities. *J Cell Biol* 86(3):831–845.
55. Yang Y, et al. (2015) Endophilin A1 regulates dendritic spine morphogenesis and stability through interaction with p140Cap. *Cell Res* 25(4):496–516.